J Fluoresc (2012) 22:1151–1158
DOI 10.1007/s10895-012-1054-0

ORIGINAL PAPER

End-to-end Distance Distribution in Fluorescent Derivatives of Bradykinin in Interaction with Lipid Vesicles

L. R. Montaldi · M. Berardi · E. S. Souza · L. Juliano · A. S. Ito

Received: 29 November 2011 / Accepted: 19 March 2012 / Published online: 10 April 2012

Abstract Cellular membranes have relevant roles in processes related to proteases like human kallikreins and cathepsins. As enzyme and substrate may interact with cell membranes and associated co-factors, it is important to take into account the behavior of peptide substrates in the lipid environment. In this paper we report an study based on energy transfer in two bradykinin derived peptides labeled with the donor-acceptor pair Abz/Eddnp (*ortho*-aminobenzoic acid/N-[2,4-dinitrophenyl]-ethylenediamine). Time-resolved fluorescence experiments were performed in phosphate buffer and in the presence of large unilamelar vesicles of phospholipids, and of micelles of sodium dodecyl sulphate (SDS). The decay kinetics were analyzed using the program CONTIN to obtain end-to-end distance distribution functions f(r). Despite of the large difference in the number of residues the end-to-end distance of the longer peptide (9 amino acid residues) is only 20% larger than the values obtained for the shorter peptide (5 amino acid residues). The proline residue, in position 4 of the bradykinin sequence promotes a turn in the longer peptide chain, shortening its end-to-end distance. The surfactant SDS has a strong disorganizing effect, substantially broadening the distance distributions, while temperature increase has mild effects in the flexibility of the chains, causing small increase in the distribution width. The interaction with phospholipid vesicles stabilizes more compact conformations, decreasing end-to-end distances in the peptides. Anisotropy experiments showed that rotational diffusion was not severely affected by the interaction with the vesicles, suggesting a location for the peptides in the surface region of the bilayer, a result consistent with small effect of lipid phase transition on the peptides conformations.

Keywords Bradykinin · Phospholipid vesicles · Forster resonance energy transfer · Distance distribution · Peptide-lipid interaction

L. R. Montaldi · M. Berardi · A. S. Ito
Departamento de Física, Faculdade de Filosofia Ciências e Letras de Ribeirão Preto, Universidade de São Paulo, São Paulo, Brazil

E. S. Souza
Departamento de Física,
Universidade Federal de Goiás—Campus Catalão,
Catalão, GO, Brazil

L. Juliano
Departamento de Biofísica, Universidade Federal de São Paulo,
Escola Paulista de Medicina,
São Paulo, Brazil

A. S. Ito (✉)
Departamento de Física, FFCLRP, Universidade de São Paulo,
Av. Bandeirantes 3900,
14040-901, Ribeirão Preto, Brazil
e-mail: amandosi@ffclrp.usp.br

Introduction

The fluorescent molecule *ortho*- aminobenzoic acid (*o*-Abz), covalently bound to the amino terminus side, combined with the acceptor group ethylene dinitrophenyl (Eddnp) linked to the carboxy terminus side of peptides generate Förster resonance energy transfer (FRET) peptides that are largely used as substrates in assays of proteases. A considerable advance in the study of proteases was possible with the use of these substrates [1, 2]: if the labeled peptide is a substrate for proteases, the fluorescence intensity increases with enzimatic hydrolysis due to the separation of donor and acceptor groups and the subsequent reduction of the energy transfer rate [3]. This method was applied, for example, in the investigation of proteases like human tissue kallikrein, through the synthesis of peptides labeled with the pair Abz-Eddnp, having the

sequence of human kininogen that spanned the region containing bradykinin (Bk) and assayed as substrates for tissue-kallikreins [3, 4].

Intramembranar proteolysis occurs in domains of transmembranar proteins which are liberated and become functional in the intra- or extra-cellular medium to perform their biological activity. The process is well regulated, triggering other physiological responses, like those associated to deposition and formation of protein plaques. Recently it has been emphasized the importance of the cellular and subcellular membranes in processes related to proteases like human kallikreins and cathepsins. For example, kallikrein secretion in cancer cells involves co-factors located in microdomains in the plasma membrane. It was also observed that the activity of kallikrein sub-types are inhibited by interaction with membrane bound lipophilic proteins [5]. As both enzyme and substrate may interact with other cell components like membranes and cell membrane associated co-factors, the involvement of such components may be relevant for the protease activity. Thus it becomes important to take into account the behavior of peptide substrates in the cell membrane and we present here results of conformational studies in bradikinin derived peptides modulated by interaction with model membranes.

The emission of *o*-Abz shows dependence with the medium polarity [6] and it was shown that, when bound to the peptide hormone braykinin and fragments, the molecule is an useful probe to monitor the peptide interaction with model membranes made by DMPG large unilamelar vesicles [7], with results comparable to those obtained by ESR techniques [8]. Bradykinin is a hormone peptide with sequence Arg-Pro-Pro-Gly-Phe-Ser-Pro-Phe-Arg, present in human body fluids, known to be involved in a variety of physiological processes, like vasodilatation, inflammation and pain [9, 10]. Conformations of the peptide have been studied by nuclear magnetic resonance (NMR) and circular dichroism (CD) spectroscopy in different solvents. It was found that the peptide and some analogs possess a large degree of conformational flexibility in aqueous medium [11, 12] and in organic solvents or in the presence of amphiphilic aggregates, folded conformations could be identified [13, 14].

In detailed studies of the energy transfer process, the application of the CONTIN program for the analysis of fluorescence decay measurements allowed obtention of complementary information to the enzimatic assays. In peptides labeled with the pair Abz-Eddnp quantitative changes in intramoleular distances were measured, reflecting conformational modifications induced by interactions with the solvent and with other molecules in the environment, like glicosaminoglicans. [15, 16]. The method was also applied to study the conformational dynamics of Abz-bradykinin-Eddnp and it was possible to verify that the bioactive hormone presents broad distribution distances in water which reflects the characteristic flexibility of the peptide. The distance distribution recovered for bradykinin in the less polar solvent TFE (Trifluoroethanol) showed the existence of two populations, indicating the decrease in the flexibility of the peptide, in agreement with the occurrence of L-turns in less polar solvents, observed using other techniques, like NMR and CD. From the study of longer and smaller derivatives of bradykinin, it is possible to draw a picture showing the importance of the proline residues in the stabilization of folded conformations of the peptide [17].

In the present work, we report measurements of time-resolved fluorescence decay of two bradykinin derived peptides labeled with the donor-acceptor pair Abz-Eddnp: Abz-SPFRQ-Eddnp and Abz-GFSPFSSRQ-Eddnp (hereafter called bkh1 and bkh2, respectively). Intensity decay was measured in phosphate buffer and in the presence of SDS micelles and of large unilamelar vesicles (LUV's) made of the anionic phospolipid DMPG and the zwitterionic DMPC, either below or above the main phase transition temperature. The complex decay kinetics were fitted to multi-exponential curves, and the data were analyzed using the program CONTIN to obtain the end-to-end distance distribution function f(r).

Material and Methods

Peptide Synthesis

The intramolecularly quenched fluorogenic peptides contain N-[2,4-dinitrophenyl]-ethylenediamine (EDDnp) attached to glutamine, a necessary result of the solid phase peptide synthesis strategy employed, the details of which are provided elsewhere [18]. An automated bench-top simultaneous multiple solid-phase peptide synthesizer (PSSM 8 system from Shimadzu) was used for the solid-phase synthesis of all the peptides by the Fmoc-procedure. The final deprotected peptides were purified by semipreparative HPLC using an Econosil C-18 column (10 W, 22.5U250 mm) and a two-solvent system: (A) trifluoroacetic acid (TFA)/H2O (1:1000) and (B) TFA/acetonitrile (ACN)/H2O (1:900:100). The column was eluted at a flow rate of 5 ml/min with a 10 (or 30) to 50 (or 60)% gradient of solvent B over 30 or 45 min. Analytical HPLC was performed using a binary HPLC system from Shimadzu with a SPD-10AV Shimadzu UV–VIS detector and a Shimadzu RF-535 Fluorescence detector, coupled to an Ultrasphere C-18 column (5 W, 4.6U150 mm) which was eluted with solvent systems A1 (H3PO4/H2O, 1:1000) and B1 (ACN/H2O/H3PO4, 900:100:1) at a flow rate of 1.7 ml/min and a 10–80% gradient of B1 over 15 min. The HPLC column eluates were monitored by their absorbance at 220 nm and by fluorescence emission at 420 nm following excitation at 320 nm. The molecular weight and purity of synthesized

peptides were checked by MALDI-TOF mass spectrometry (TofSpec-E, Micromass) and by peptide sequencing using a protein sequencer PPSQ-23 (Shimadzu Tokyo, Japan).

Materials

The phospholipids DMPC (1,2-dimyristoyl-*sn*-glycero-3-phosphocholine) and DPPC (1,2-dipalmitoyl-*sn*-glycero-3-phosphocholine) and the sodium salt of the phospholipid DMPG (1,2-dimyristoyl-*sn*-glycero-3-phospho-*rac*-glycerol) were purchased from Avanti Polar Lipids (Birmingham, AL, USA). Other reagents, used without additional purification, were obtained from Sigma Chemical Co. (St. Louis, MO, USA). The phosphate buffer was used at the concentration of 10 mM, adjusted with NaOH to pH 7.4.

Vesicles Preparation

Lipid vesicles were prepared by the method of extrusion. A lipid film was formed from a chloroform solution of lipids, dried under a stream of N_2, and left under reduced pressure for a minimum of 2 h, to remove all traces of the organic solvent. The film was re-suspended in phosphate buffer by vortexing, to a concentration of 1 mM. The suspension was then extruded through polycarbonate membranes at temperatures above the gel to fluid phase transition. The extrusion final step consisted in the use of 0.1 μm pore diameter polycarbonate membranes, resulting in large unilamellar vesicles (LUV).

Optical Absorption and Fluorescene Measurements

Stock solutions of peptides were prepared in (buffer). Optical absorption and fluorescence measurements were made dissolving the stock in phosphate buffer, pH 7.4 to final peptide concentrations between 2×10^{-5} and 4×10^{-5} M.

Optical absorption measurements were performed using an Amersahm-Pharmacia 2100 Ultraspec array spectrophotometer. A Hitachi F-7000 spectrofluorimeter, with polarizer filters for anisotropy experiments, was used for steady state fluorescence measurements. Excitation and emission slits of 1 nm or 2 nm bandpass were used, depending on the fluorescence intensity of the sample. The temperature was controlled with a Julabo F25 refrigerated circulating bath.

Fluorescence decays and time-resolved anisotropy were measured in an apparatus based on the time-correlated single photon counting method. The excitation source was a Tsunami 3950 Spectra Physics titanium-sapphire laser, pumped by a Millenia X Spectra Physics solid state laser. The repetition rate of the pulses was set to 8.0 MHz using the 3980 Spectra Physics pulse picker. The laser was tuned so that a third harmonic generator BBO crystal (GWN-23PL Spectra Physics) gave the 310 nm excitation pulses that were directed to an Edinburgh FL900 spectrometer. The spectrometer was set in L-format configuration, the emission wavelength was selected by a monochromator, and emitted photons were detected by a refrigerated Hamamatsu R3809U microchannel plate photomultiplier. Soleil-Babinet compensator in the excitation beam and Glann-Thomson polarizer in the emission beam were used in anisotropy experiments. The FWHM of the instrument response function was typically 100 ps and time resolution was 12 ps per channel and a software provided by Edinburgh Instruments was used to analyze the individual decays, which were fitted to multi-exponential curves.

$$I(t) = \sum \alpha_i e^{(-t/\tau_i)} \tag{1}$$

where α_i and τ_i are pre-exponential factor and lifetime of the component *i* of decay. The quality of the fit was judged by the analysis of the statistical parameter reduced-χ^2 and by inspection of the residuals distribution.

Computation

For a single fixed distance *r* between donor and acceptor, the energy transfer rate (k_T) is given by $k_T = R_o^6/\tau_d r^6$ where R_o is the Förster distance, that is dependent on the spectral overlap between donor's emission and acceptor's absorption, and τ_d is the donor's lifetime . It results from the model that the additional route for deexcitation affects the fluorescence decay of the donor, and the time evolution of the fluorescence intensity turns out to be given by

$$I(t) = I_0 \exp\left[\left(-\frac{1}{\tau_d} - \frac{R_0^6}{\tau_d r^6}\right)t\right] \tag{2}$$

Equation (2) fails to fit to the experimental decay when more than one distance is present during the lifetime of the fluorophore. A distance distribution, represented by a function *f(r)*, can be recovered from the experimental decay data by the use of the CONTIN program [Provencher, 1982] that inverts general systems of linear algebraic equations of the type

$$y(t_k) = \int_a^b f(r)K(r,t_k)dr + \sum_{j=1}^{N_L} L_{kj}\beta_i\,,\ k = 1,.....N_y \tag{3}$$

where $y(t_k)$ corresponds to the measured intensity of fluorescence at the instant t_k. The distance distribution function *f(r)* is recovered within a chosen interval r, initially set between 5 and 45 Å , divided in N equally spaced intervals, and the integral is converted, by numerical integration, to a summation in r_j . The function inside the integral is then written as $K(r_j, t_k)$ and corresponds to Eq. (2), written for the instant t_k , deconvoluted from the instrument response function, and assumed to be valid for each distance r_j within the chosen interval.

The second term in Eq. (3) accounts for impurities that may be present contributing to the decay profile. The program recovers the parameter β_j corresponding to the contribution L_{kj} of the jth impurity to the fluorescence intensity at the instant t_k. In the analysis we also imposed the constraint of non-negativity for the distribution function. The best solution was found using the weighted leastsquares method with the employment of a regularizor based on the principles of parsimony [19].

The distance R_o used in equation for the function $K(r_j, t_k)$, was obtained from the spectral data of the donor's emission $F_d(\lambda)$ and acceptor's extinction coefficient for absorption $\varepsilon_a(\lambda)$, through

$$R_o^6 = \frac{9000(\ln 10)\kappa^2 \Phi_d}{128\pi^5 n^4 N_0} \int F_d(\lambda)\varepsilon_a(\lambda)\lambda^4 d\lambda \quad (4)$$

where n is the refractive index of the medium, Φ_d is the quantum yield of the donor and κ is the orientational term dependent on the relative angles between dipoles moments from donor and acceptor.

Results and Discussion

Peptides in Aqueous Medium

The optical absorption spectra of Abz labeled bradykinin (Abz-BK-NH_2) and other small peptides like Abz-LRF-NH_2, Abz-FRPR-NH_2 and Abz-FRRPR-NH_2 in aqueous medium present a near-UV band centered around 315 nm and the emission band has maximum intensity around 420 nm [18, 20]. Similar results were obtained for the monoamino derivative Abz-$NHCH_3$ [21] and their spectroscopic properties like absorption and emission spectra and fluorescence lifetime were used as representative of the Abz labelled peptides without the acceptor group Eddnp.

From time-resolved fluorescence experiments in buffer solution, we verified that the intensity decay profiles of the peptides without the acceptor group were practically monoexponential, dominated by lifetimes near to 8.0 ns, that accounts for 97% of the total emission (Fig. 1). The decay profile of the peptides containing the donor-acceptor are drastically changed (Fig. 1). The proximity between donor and acceptor strongly reduces the excited state lifetime and the decay could not be fitted to a monoexponential curve, suggesting the occurrence of several separation distances between donor and acceptor in the peptides.

The steady state anisotropy for the peptide bkh2 in buffer at 20 °C (Table 1) is comparable to that obtained for Abz-bk, the peptide containing only the donor group [7]. From the dimensions of the peptides one should expect higher values of steady state anysotropy for the longer peptide. However the measurements resulted in higher anisotropy for the shorter peptide (Table 1). Due to the fast initial intensity decay of peptide bkh1, the deexcitation occurs before the depolarization driven by rotational effects had time to manifest, leading to higher values of steady state anisotropy, compared to those that can be obtained when the fluorophore remains in the excited state during a time long enough to rotate. Time resolved anisotropy decays were fitted to small values of rotational correlation times, in the order of hundred picoseconds. The values are not strictly corresponding to rotational

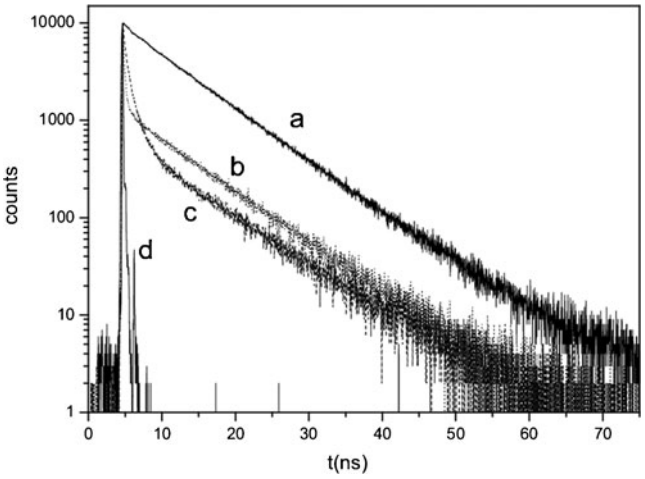

Fig. 1 Intensity decay for Abz labeled peptides: **a** Abz-bk, **b** bkh1, **c** bkh2 in buffer 18 °C. Also shown the instrument response function **d**

Table 1 Steady state anisotropy (r), rotational correlation time Φ and limiting or residual anisotropy (r_∞) for peptides bkh1 and bkh2 in buffer and in the presence of vesicles and micelles

	bkh1			bkh2		
	r	Φ (ns)	r_∞	r	Φ (ns)	r_∞
buffer						
20 C	0,022	0,29	−0,007	0,014	0,31	−0,010
30 C	0,013	0,23	0,006	0,008	0,20	−0,004
40 C	0,011	0,19	−0,003	0,007	0,21	−0,001
50 C	0.013	0,18	0,007	0,008	0,17	−0,011
DMPC						
18 C	0,074	0,28	−0,020	0,039	0,46	0,023
30 C	0,056	0,33	0,005	0,043	0,39	−0,006
DMPG						
18 C	0,017	0,34	0,035	0,042	0,58	0,004
30 C	0,020	0,37	0,007	0,032	0,77	−0,006
DPPC						
40 C	0,095	0,27	0,001	0,036	0,50	−0,001
50 C	0,091	0,61	0,007	0,035	0,32	−0,001
SDS						
20 C	0,022	1,36	−0,005	0,046	1,67	−0,008

diffusion because of the contribution of the energy transfer to depolarization. From the data it was not possible to discriminate between those different contributions to depolarization and the anisotropy decay, for both peptides, was fitted to a monoexponential curve. In buffer, the decrease in steady-state anisotropy and rotational correlation times when the temperature raises, is consistent with the randomization promoted by increase in thermal effects. Within experimental uncertainties, the residual anisotropy is close to zero, indicating that both peptides are free to rotate in buffer solution.

The intensity decay profiles were analysed within the framework of Forster Resonance Energy Transfer processes. Initially the superposition integral which appears in Eq. (3) was calculated from the emission spectrum of Abz-bk and the absorption spectrum of the acceptor Eddnp (Fig. 2). The quantum yield of the donor, was obtained using the value 0.6 in ethanol as reference [17] and assuming the value 2/3 for the orientational term, which represent a mean value for the relative orientation of donor and acceptor electric dipoles, the Forster distance for the Abz/Eddnp pair in buffer was calculated as 32 Å,. The use of the Contin program allowed us to obtain the distribution of donor-acceptor distances which represents the end-to-end distances of the peptides in buffer solution (Fig. 3). The small peptide bkh1 has 5 amino acid residues while the longer peptide bkh2 has 9 residues. However the distance distributions reveal that the end-to-end separation for the longer peptide is only slightly higher: in bkh1 there is a predominant end-to-end distance around 16 Å, while in bkh2 two equally populated distributions are present, around 17 Å and 23 Å, showing the existence of an equilibrium between two conformations for that peptide. The proline residue in position 4 of bradykinin sequence, promotes a turn in the structure, thus shortening the end-to-end distance of the long peptide bkh2.

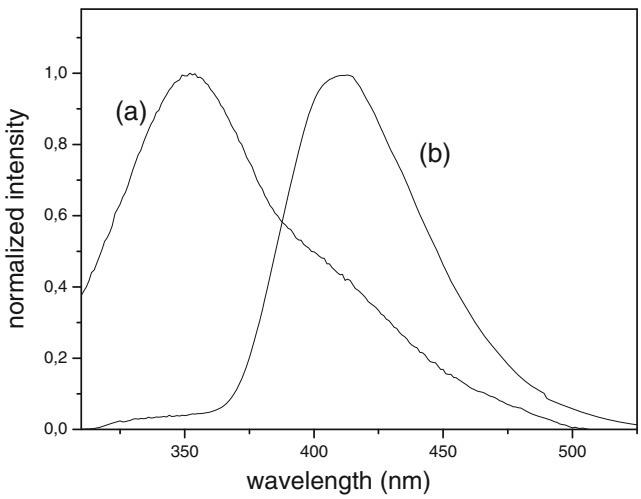

Fig. 2 Spectral superposition of Eddnp absorption **a** and Abz-bk emission **b**, with excitation at 315 nm, in phosphate buffer 0.010 M, 20 °C. Spectra are normalized to unity at absorption or emission peaks

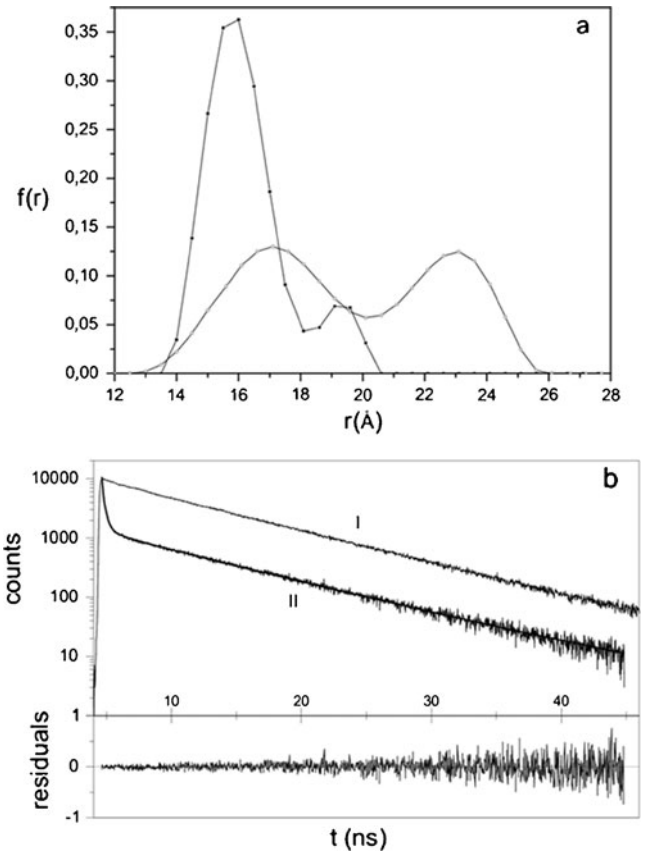

Fig. 3 **a** Distance distribution for bkh1 (*filled square*) and bkh2 (*empty circle*) in buffer 18 °C, recovered from intensity decay using CONTIN program. **b** Also shown decay and fit for *(I)* Abz-bk and for bkh1 *(II)* and plot of residuals for bkh1

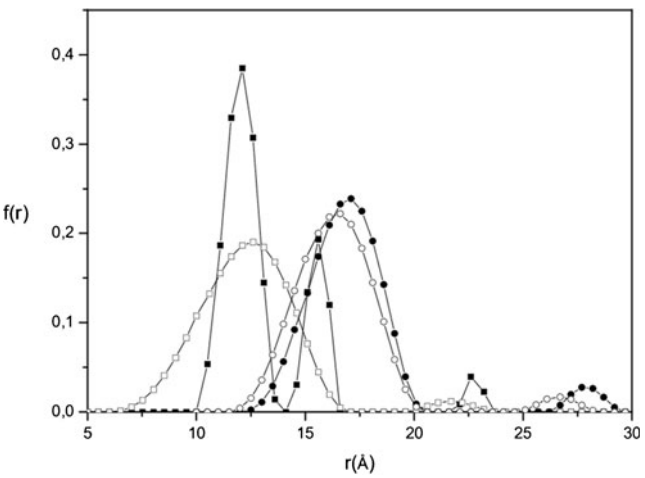

Fig. 4 Distance distribution for bkh1 in the presence of vesicles of (*empty square*) DMPG (1 mM), (*filled square*) DMPC (1 mM), (*filled circle*) DPPC (1 mM) and (*empty circle*) SDS micelles (30 mM), recovered from intensity decay using CONTIN program. Temperature 18 °C; for DPPC, temperature 40 °C

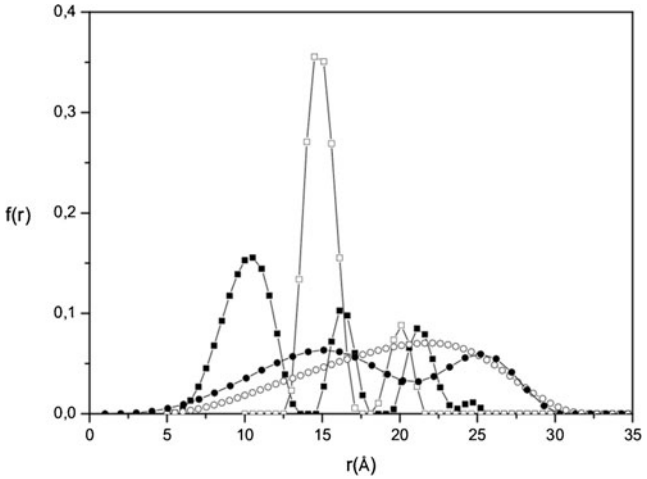

Fig. 5 Distance distribution for bkh2 in the presence of vesicles of (*empty square*) DMPG (1 mM), (*filled square*) DMPC (1 mM), (*filled circle*) DPPC (1 mM) and (*empty circle*) SDS micelles (30 mM), recovered from intensity decay using CONTIN program. Temperature 18 °C; for DPPC, temperature 40 °C

Peptides in Micelles and Vesicles

Experiments on the interaction of peptides with lipids were carried out adding small amounts of peptide to concentrated lipid vesicle dispersion (1 mM). At such peptide/lipid concentrations (30 μM/ 1.0 mM) it was observed that peptides like Abz-BK-NH_2 were completely bound to DMPG vesicles [7], with a small shift of the fluorescence emission spectrum to lower wavelengths (412 nm). The decay kinetics of the peptide containing only the donor was also practically mono exponential, with the main lifetime around 8.0 ns. For the peptides containing the donor-acceptor pair in the presence of vesicles or micelles the intensity decays were heterogeneous and could not be fitted to mono exponential curves.

The steady state anisotropy of bkh1 and bkh2 increased in the presence of vesicles and micelles (Table 1), indicating that the peptides inserts into the membranes, decreasing its mobilility. For the small peptide bkh1 the changes are more pronounced whit vesicles of zwitterionic lipids DMPC and DPPC compared to the acidic DMPG, while in bkh2 the increase in the anisotropy was similar for the three lipids. The additional Arg residue in bkh2 may help its interaction with the negative vesicles of DMPG.

Taking into account the absorption and emission spectra and the values of the donor quantum yield determined in the presence of the model membranes, the Forster distances were re-calculated, and the values obtained were 30 Å in phosphate buffer containing 1 mM DMPG or DMPC, 37 Å in DPPC 1 mM and 39 Å in SDS 30 mM. Using similar procedure employed in the analysis of the peptides in buffer, the CONTIN program was used to recover Abz-Eddnp distance distributions in the peptides in interaction with vesicles and micelles (Figs. 4 and 5). We observed that the surfactant SDS, above the critical micelar concentration has a disorganizing effect, broadening the distance distributions. The effect is particularly strong for the long peptide bkh2, where the end-to-end distances can extend to values as long as 30 Å, and the two conformations observed in buffer are no longer clearly discernible. The end-to-end distance distributions of the peptides in the vesicles are considerably different from those observed in phosphate buffer (Table 2). The peptides acquire more compact conformation as verified by the shortening of the end-to-end distance of the peptides in interaction with the lipid bilayer. The two

Table 2 Results of distance distribution recovered from intensity decay using CONTIN program: position of the peaks of distributin (r_i) and corresponding full width at half maximum (σ_i) and fractional contribution to the total distribution (f_i). *Obs.: A third peak appears for bkh1 in DMPC 18 °C at 22,6(1,0) Å with 3,8% contribution, and for bkh2 in: DMPC 18 °C at 21,1(2,0) Å with 18,1%, and DMPC 30 °C at 20,7(2,5) Å with 28,5% contribution

	bkh1				bkh2			
	r_1 (σ_1) Å	f_1	r_2 (σ_2) Å	f_2	r_1 (σ_1) Å	f_1	r_2 (σ_2) Å	f_2
buffer								
18 °C	16(2,4)	88,2	19,1(2,0)	11,8	17,1(4,5)	55,5	23,1(3,8)	44,5
30 °C	15,5(3,3)	98,1	20,1(1,5)	1,9	16,6(2,0)	49,7	22,1(3,0)	50,3
40 °C	15,1(3,4)	100,0			16,5(2,6)	49,0	21,1(3,2)	51,0
DMPC								
18 °C	12,1(1,8)	72,3	15,6(1,2)	23,9	10,5(3,9)	61,5	16,1(1,8)	18,9
30 °C	11,1(3,1)	96,4	22,2(1,3)	3,6	11,1(4,4)	41,7	15,7(3,5)	29,8
DMPG								
18 °C	12,6(5,1)	97,2	21,7(2,0)	2,8	14,5(2,3)	84,6	20,1(1,7)	15,4
30 °C	12,6(4,3)	96,7	21,6(2,0)	2,8	14,6(4,9)	88,7	20,6(2,8)	11,3
DPPC								
40 °C	17,1(3,9)	94,8	27,7(1,9)	5,2	15,1(10,6)	65,5	25,2(6,7)	34,5
50 °C	17,2(4,9)	94,9	28,9(2,6)	5,1	11,1(13,4)	61,1	24,2(9,4)	38,9
SDS								
20 °C	16,6(4,3)	96,6	26,7(2,0)	3,4	21,6(14,2)	100,0		

conformations of peptide bkh1 merge to one conformation in DMPG and in DPPC (either in gel as in liquid crystalline phase). On the other hand, in interaction with vesicles of DMPC, the long peptide bkh2 presents three groups of distance distributions, indicating a partition between water and vesicles such that a fraction of peptides remains in the aqueous environment.

It has to be noticed also that the increase in temperature, which promotes phase transitions in the phospholipid vesicles, do not affect the position of the peaks in the distribution of distances of the short peptide bkh1 and the main effect is to increase the width of the distribution. The same was observed for bkh2 in vesicles of DMPG. However, in vesicles of DMPC the increase in temperature leads to the decrease in the population of peptides with short distances while in DPPC there is a significative broadening in the distributions.

Conclusions

Despite of the fact that bkh2 has 9 amino acid residues, its end-to-end distance is no more than 20% longer than the values obtained for bkh1 which has 5 amino acids. The proline residue, in position 4 of the amino acid sequence of bkh2, promotes a turn in the peptide chain, resulting in the shortening of the end-to-end distances. The occurrence of two conformational families are ascribed to the two possibilities for the dihedral angle corresponding to the linkage of proline to the subsequent phenylalanine residue.

Higher temperatures increases the flexibility of the chains, as observed by the broadening in the distribution width. A strong disorganizing effect is promoted by the surfactant SDS, which substantially enlarges the distances and broadens the distributions. The interaction with phospholipid vesicles makes the chains more compact and end-to-end distances in the peptides decreases. In addition, in DMPC vesicles three distinct populations are distinguished in the long peptide bkh2, revealing partition of the peptides between the vesicles and the aqueous phase. Anisotropy results indicate that rotational constraints are not enhanced by the interaction with the bilayers, suggesting that peptides locate in the surface region of the vesicles. The result is consistent with the small effect of lipid phase transition on the peptides conformation.

On the grounds of the importance of the cellular and subcellular membranes in processes related to proteases, like intermebranar proteolysis, the interaction of substrates with the lipid phase may promote conformational constraints that can be relevant to the enzyme activity. We observed that indeed these structural changes are present in the interaction of bradikynin derivatives with different kinds of phospholipid vesicles and the fluorescence energy-transfer can be used to quantify the changes, by the determination of end-to-end distances distributions.

Acknowledgments We thank the Brazilian agencies FAPESP and CNPq for financial support. MB and LMR thanks FAPESP and CNPq for fellowships. Support from INCT-FCx, Brazil, is also acknowledged.

References

1. Carmona AK, Schwager SL, Juliano MA, Juliano L, Sturrock ED (2007) A continuous fluorescence resonance energy transfer angiotensin I-converting enzyme assay. Nat Protoc 1:1971–1976
2. Korkmaz B, Attucci S, Juliano MA, Kalupov T, Jourdan ML, Juliano L, Gauthier F (2008) Measuring elastase, proteinase 3 and cathepsin G activities at the surface of human neutrophils with fluorescence resonance energy transfer substrates. Nat Protoc 3:991–1000
3. Chagas JR, Portaro FC, Hirata IY, Almeida PC, Juliano MA, Juliano L, Prado ES (1995) Determinants of the unusual cleavage specificity of lysyl-bradykinin-releasing kallikreins. Biochem J 306:63–69
4. Del Nery E, Chagas JR, Juliano MA, Prado ES, Juliano L (1995) Evaluation of the extent of the binding site in human tissue kallikrein by synthetic substrates with sequences of human kininogen fragments. Biochem J 312:233–238
5. Henkhaus RS, Roy UKB, Cavallo-Medved D, Sloane BF, Gerner EW, Ignatenko NA (2008) Caveolin-1-Mediated Expression and Secretion of Kallikrein 6 in Colon Cancer Cells. Neoplasia 10:140–148
6. Takara M, Ito AS (2005) General and specific solvent effects in optical spectra of ortho-aminobenzoic acid. J Fluoresc 15:171–177
7. Turchiello RF, Lamy-Freund MT, Hirata IY, Juliano L, Ito AS (2002) Ortho-Aminobenzoic Acid-Labeled Bradykinins in Interaction with Lipid Vesicles: Fluorescence Study. Biopolymers 65:336–346
8. Turchiello RF, Juliano L, Ito AS, Lamy-Freund MT (2000) How bradykinin alters the lipid membrane structure. A spin label comparative study with bradykinin fragments and other cations. Biopolymers 54:211–221
9. Regoli D, Barabe J (1980) Pharmacology of bradykinin and related kinins. Pharmacol Rev 32:1–46
10. Stewart JM (1995) Bradykinin antagonists: development and applications. Biopolymers 37:143–155
11. Cann JR, Stewart JM, Matsueda GR (1973) A circular dichroism study of the secondary structure of bradykinin. Biochemistry 12:3780–3788
12. Denys L, Bothner-By AA, Fisher GH, Ryan JW (1982) Conformational diversity of bradykinin in aqueous solution. Biochemistry 21:6531–6536
13. Cann JR, Liu X, Stewart JM, Gera J, Kotovych GA (1994) CD and NMR study of multiple bradykinin conformations in aqueous tri-£uoroethanol solutions. Biopolymers 34:869–878
14. Kotovych G, Cann JR, Stewart JM, Yamamoto H (1998) NMR and CD conformational studies of bradykinin and its agonists and antagonists: application to receptor binding. Biochem Cell Biol 76:257–266
15. Ito AS, Souza ES, Barbosa SR, Nakaie CR (2001) Fluorescence study of conformational properties of melanotropins labeled with aminobenzoic acid. Biophys J 81:1180–1189
16. Pimenta DC, Nantes IL, Souza ES, le Boniec B, Ito AS, Tersariol ILS, Oliveira V, Juliano MA, Juliano L (2002) Interaction of

heparin with internally quenched fluorogenic peptides derived from heparin-binding consensus sequences, kallistatin and antithrombin III. Biochem J 366:435–446
17. Souza ES, Hirata IY, Juliano L, Ito AS (2000) End-to-end distribution distances in bradykinin observed by fluorescence energy transfer. Bioch Biophys Acta 1474:251–261
18. Ito AS, Turchiello RF, Hirata IY, Cezari MH, Meldal M, Juliano L (1998) Fluorescent properties of amino acids labeled with orthoaminobenzoic. Biospectroscopy 4:395–402
19. Provencher SW (1982) CONTIN: a general purpose constrained regularization program for inverting noisy linear algebraic and integral equations, Computer Phys. Commun 27:229–242
20. Turchiello RF, Lamy-Freund MT, Hirata IY, Juliano L, Ito AS (1998) *ortho*-aminobenzoic acid as a fluorescent probe for the interaction between peptides and micelles. Biophys Chem 73:217–225
21. Takara M, Eisenhut JK, Hirata IY, Juliano L, Ito AS (2009) Solvent effects in optical spectra of ortho-Aminobenzoic acid derivatives. J Fluoresc 19:1053–1060